Research Article

Study on the Load Transfer Behaviour and Bond-Slip Model of Fully Grouted Rockbolt

Shuisheng Yu [ID],[1] **Honghao Yang** [ID],[1] **Jin Chen** [ID],[2] **Yawei Wang** [ID],[1] **and Shucan Lu** [ID][1]

[1]*School of Architectural Engineering, Zhongyuan University of Technology, Zhengzhou 450007, China*
[2]*School of Economics and Management, Zhongyuan University of Technology, Zhengzhou 450007, China*

Correspondence should be addressed to Shuisheng Yu; yuss.1987@163.com

Rockbolts are often subjected to loads during service, and the load transfer behaviour of rockbolts is very important. Therefore, in this study, pullout tests were performed on two kinds of rockbolt systems, with and without defects, and the load transfer behaviour and failure modes were analysed. According to the load transfer process between the rockbolt and cement mortar interface, a bond-slip model considering the yield of the rockbolt was proposed, and the nonlinear behaviour in the softening stage was considered. The test results showed that the evolution of the interface load between the rockbolt and cement mortar in the grouted rockbolt systems without defects underwent four stages of gradual failure, namely, elasticity, yield, softening, and complete slip, and its failure mode involved the rockbolt being pulled out accompanied by splitting cracks and tensile cracks on the concrete surface. The proposed bond-slip models considering the nonyielding and yielding of the rockbolt can accurately reflect the actual load transfer behaviour of a fully grouted rockbolt.

1. Introduction

Rockbolt support systems involve a simple structure and extensive support form and have the advantages of high support strength, low cost, and good supporting effect. Furthermore, they can make full use of the surrounding rock to bear the load, maximally maintain the integrity and stability of the surrounding rock, effectively control the development of deformation, displacement, and cracks in the surrounding rock, and provide support to the surrounding rock itself [1]. Hence, such systems are widely used in various fields, such as underground engineering. During the service period, rockbolts are often subjected to different loads, and the propagation of the loads in the rockbolts is a very complex process. For decades, many scholars have conducted extensive research on the load transmission behaviour of rockbolts [2–9]. Sun et al. [2] considered the installation time and the length of the rockbolt, analysed the displacement process of a deep tunnel, and showed that increasing the length of the rockbolt from 2 m to 4 m in a 14 m high tunnel could reduce the tunnel wall

displacement by 20%. Spearing et al. [3] proposed a new method to test the performance of field rockbolts, namely, evenly staggering the placement of strain gauges on rockbolts to measure the axial stress change of the rockbolts. Bae et al. [4] studied the influence of different concrete strengths, thicknesses, and steel fibre contents on the bonding strength of reinforced active powder concrete. The results showed that the growth rate of the bond strength decreased with increasing concrete compression strength, and the damage mode of specimens changed with increasing steel fibre content. The bonding strength increased, but the growth rate was different. Luga and Periku [5] studied the bearing capacity of rockbolts by conducting an in situ pullout test in the field, and the results showed that the anchorage strength and displacement of the rockbolt decreased with increasing horizontal mounting angle. Thenevin et al. [6] studied the influence of the anchorage pressure and anchorage length on the load. Teymen and Kilic [7] investigated the effect of the anchorage strength on the stress distribution in a full-length rockbolt and showed that the stress distribution on the rockbolt was more uniform with increasing anchorage

strength and stiffness. Khaleghparast et al. [8] studied the shear strength of rockbolts under static and dynamic loading. The results showed that using perforated steel tubes inside concrete blocks as internal confinement in the vicinity of shear planes prevented axial and radial cracking in the concrete, which enabled the rockbolt to undergo more shear than tension. Furthermore, the shear performance of a conventional rockbolt under a high-velocity impact load was found to be 70% of that under static loading conditions. Yu et al. [9] studied the damage mode of rockbolts and the damage process of the anchor structure through test and numerical simulation methods. The results showed that with increasing anchor length, the damage process of the rockbolt anchor system finally occurred at the loading end and the free end. In conclusion, although some scholars studied the load transfer behaviour of rockbolts, their research was not sufficiently comprehensive and failed to assess whether grouted rockbolt systems contained defects that could affect the load transfer behaviour of grouted rockbolt systems.

The key problems in studying the rockbolt anchorage mechanism include choosing a reasonable bond-slip model, simplifying the anchorage problem, and accurately reflecting objective reality. Many scholars have studied the bond-slip model, and an ideal elastic plastic bond-slip model has been used by many commercial software developers to study the mechanical behaviour of rockbolts, but this model does not consider the interfacial softening phenomenon [10]. The test results of Hawkes and Evans indicated that the interfacial shear stress was nonlinear in the softening stage [11]. Benmokrane et al. [12] proposed a classic three-line model of pulling by analysing many laboratory tests. This model considered the residual strength of the rockbolt and could describe the strain-softening behaviour of the rockbolt. Monti et al. [13] proposed a bilinear bond-slip model, which overcame the main defect of the ideal elastic-plastic model as it reflected slip softening in a linearly decreasing manner, but it failed to describe the debonding behaviour of the anchor-anchorage interface. Trabacchin et al. [14] used theories and tests to analyse the bonding behaviour between basalt FRP (fibre-reinforced polymer) bars and concrete and proposed a bilinear bond-slip model. Ren et al. [15] considered the residual bond strength and proposed an analytical solution to predict the mechanical properties of a full-length rockbolt during pulling based on the three-length bond-slip model. Shen et al. [16] studied the bonding performance between early high-strength concrete and reinforcement by using the pullout test and proposed a model to predict the bonding strength-slip interaction relationship between concrete and reinforcement in the early stage, which was in good agreement with test results. Zhou et al. [17] studied the double exponential curve shear slip model and the rockbolt linear reinforcement elastic-plastic constitutive model based on numerical modelling. Based on the results of a pullout test, the numerical model could well describe the rockbolt interfacial slip failure and tensile failure as two forms of damage under a pullout load. Based on classical three-line models, many scholars proposed various bond-slip models, but all were based on linear softening, which overestimated the rockbolt carrying capacity [15, 18–21]. Although Yue

et al. [22] considered the load transfer behaviour of the rockbolt-anchorage interface as exponential softening, they did not consider the situation of the rockbolt yielding under a pullout load. Chen et al. [23] studied the bond properties and bond-slip constitutive model of reinforcement in rubber powder-modified polypropylene fibre concrete, but this model also did not consider the yield of the reinforcement. Many rockbolt bond-slip models consider that the rockbolt does not yield. However, when the grouted length is sufficiently long, the rockbolt yields in the pullout test, and such models cannot accurately describe rockbolt load transfer behaviour.

In view of the above problems, pullout tests of grouted rockbolt systems with and without bond defects were conducted, and the load transfer behaviour and specimen failure mode were analysed. Then, based on the load transfer process at the interface between the rockbolt and cement mortar, bond-slip models considering rockbolt nonyielding and yielding were proposed and verified by experiments. This model has a certain reference value for the study of the load transfer behaviour of rockbolts.

2. Test Arrangement

2.1. Specimen Design. In this paper, C40 concrete is used to simulate the surrounding rock. The concrete specimen is a cylinder with a diameter and length of 150 mm and 1500 mm, respectively. The raw materials are 42.5 grade ordinary Portland cement, fine aggregate comprising natural river sand with particle sizes of 0.3–1.18 mm, and coarse aggregate comprising pebbles with particle sizes of 5–20 mm. The mixture ratio of the concrete specimen is cement : water : river sand : pebbles = 1 : 0.47 : 1.3 : 3.02. Cement mortar is used as the cement mortar, and its raw materials are 42.5 grade ordinary Portland cement and fine aggregate comprising natural river sand with particle sizes of 0.3–0.6 mm [9]. To ensure that the rockbolt slips and cement mortar is easily injected into the anchor hole under the condition that the rockbolt is not pulled off, the mixture ratio of the cement mortar is water : cement : river sand = 1 : 1 : 3.2. The combination of cement mortar and concrete is shown in Table 1 [9].

The rockbolt is made of a threaded steel bar with a diameter of 25 mm and a length of 2500 mm. The concrete specimen is a cylinder with an inner diameter of 40 mm, an outer diameter of 150 mm, and a height of 1500 mm. A detailed picture of the specimen is shown in Figure 1. To simulate the field conditions, the production process of the specimen is as follows: first, a round steel bar with a diameter of 40 mm is placed in the centre of the steel mould, and concrete is poured and simultaneously vibrated to discharge the air bubbles in the concrete. After curing the concrete specimen for 2 days, the round steel bar is pulled out, and the specimen is demoulded and cured in the laboratory for 28 days until its strength is stable. Finally, cement mortar is used to anchor a rockbolt in the centre of the hole. A bond defect with a length of L was set 400 mm from end A [24], and the specimen was cured for 7 days prior to the pullout test.

TABLE 1: Mix proportions of concrete and cement mortar in test [9].

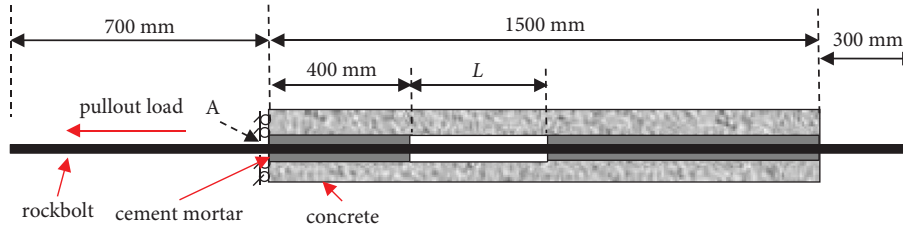| Ingredient	Water	Cement	Sand	Stone
Concrete	0.47	1	1.3	3.02
Cement mortar	1	1	3.2	0

FIGURE 1: Schematic of the grouted rockbolt systems model with bond defect.

A pullout testing machine (PTM) (see Figure 2) was designed and manufactured to conduct the rockbolt pullout test [25]. The pullout load was applied to the rockbolt by a hollow jack with a 300 kN loading capacity, and the load was measured by the load transducer. The displacement of the rockbolt was measured by the laser displacement sensor.

3. Experimental Results and Discussion

3.1. Analysis of the Load Transfer Behaviour of the Rockbolt. When the value of L is 0 mm, there is no bond defect in the grouted rockbolt systems, and the axial load transfer behaviour of the rockbolt in the grouted rockbolt systems is shown in Figure 3. During the pullout process, the rockbolt experienced four stages of progressive failure, including elasticity, yield, interface softening, and complete slip. This is mainly due to the perfect bond between the rockbolt and cement mortar. The load-displacement curve starts to rise with a high initial slope at first. The interface between the rockbolt and cement mortar is in the elastic stage, and the chemical adhesion and mechanical interlocking have not been disturbed. With increasing pullout loads, chemical adhesion and mechanical interlocking are fully mobilized and used in grouted rockbolt systems. When the shear force exceeds the shear strength of the interface between the rockbolt and cement mortar, the interface softens and gradually begins to slip. Due to the large pullout load, the rockbolt yields, but the pullout load does not reach the ultimate strength of the rockbolt. The rockbolt is not pulled out. Then, the interface bond between the rockbolt and cement mortar fails, resulting in the rockbolt completely slipping. Due to the friction between the rockbolt and cement mortar, the rockbolt has residual strength and retains a certain supporting ability.

When the value of L is 400 mm, there is a bond defect with a length of 400 mm in the grouted rockbolt systems. The axial load transfer behaviour of the rockbolt in the grouted rockbolt systems is shown in Figure 4. Due to the presence of bond defects, the rockbolt does not yield. With the increase in pullout load, the load in the rockbolt increases linearly to the maximum load, and then, the interface between the rockbolt and cement mortar softens, leading to a decreasing load, and finally, the rockbolt slips.

3.2. Failure Mode Analysis of the Grouted Rockbolt Systems. The failure mode of the grouted rockbolt systems when the value of L is 400 mm is shown in Figure 5(a), and the rockbolt is directly pulled out from the grouted systems. In the pullout process, the radial pressure on the concrete caused by the wedge action of the rockbolt is less than the tensile strength of the concrete, resulting in no damage to the surface of the concrete. The failure mode of the specimen of the grouted rockbolt systems involves the rockbolt being pulled out.

The failure mode of the grouted rockbolt systems when the value of L is 0 mm is shown in Figure 5(b). With the increase in load, the cement mortar at the loading end is first damaged and then crushed by the internal pressure of the concrete. The cement mortar first breaks at the loading end, and the surface of the rockbolt rib falls from the cement mortar. The chemical adhesive force gradually decreases, and then, the cement mortar is crushed by the internal pressure of the concrete. After the slip of the rockbolt, the cement mortar debris slides out from the grouted hole at the loading end without gathering. Therefore, the load acting on the concrete at the grouted hole at the loading end is relatively small, and the concrete does not experience splitting failure. With a further increase in the pullout load at the free end, the force acting on the free end of the rockbolt gradually increases. The sliding part of the rockbolt gradually advances towards the free end, inducing the rib of the rockbolt to crush the cement mortar, which accumulates in the grouted hole. This causes a wedge action and internal radial pressure on the concrete, resulting in radial expansion of the concrete, as shown in Figure 6 [26]. When the radial pressure exceeds the tensile strength of the concrete, internal cracks rapidly develop and spread to the surface of the concrete. However, as the free end is restricted by the end cap of the equipment, it is equivalent to exerting lateral pressure on the free end. This prevents the expansion of the concrete and finally leads to the formation of splitting cracks and tensile cracks in the middle of the concrete, which extend to the loading end. The splitting failure mode is mainly caused by the shear dilatancy of cement mortar as a result of the wedging action of the rib on the rockbolt. When the ribbed rockbolt moves under the pullout load, the cement mortar around the rockbolt undergoes shear dilatation, resulting in an increase in the radial
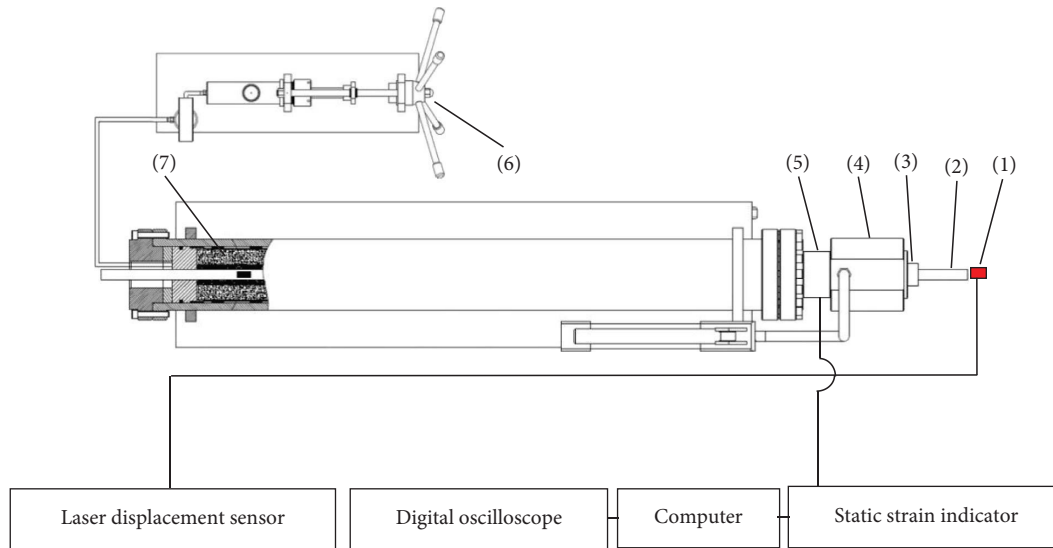
Figure 2: The schematic diagram of pullout testing machine (PTM) [25]. (1) Laser displacement sensor; (2) rockbolt; (3) anchorage device; (4) hollow jack; (5) load transducer; (6) hydraulic pump; (7) concrete specimen.
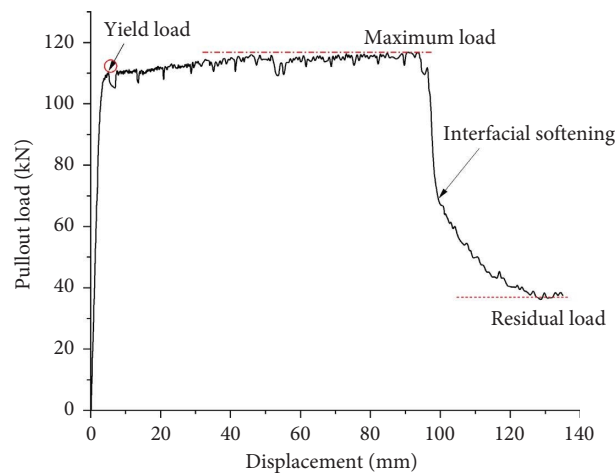

Figure 3: Axial load transfer behaviour on rockbolt when the value of L is 0 mm.

4. Determination and Test Verification of the Bond-Slip Model of a Fully Grouted Rockbolt

4.1. Determination of the Bond-Slip Model of a Fully Grouted Rockbolt. The existing trilinear bond-slip model cannot well reflect the nonlinear characteristics of the load-displacement relationship at the grouted interface [15, 18–21], while the nonlinear bond-slip model considering nonlinear softening displacement of the cement mortar [27, 28]. Figure 5(b) shows that there are four tensile cracks in the free-end concrete. After the end cover of the equipment is removed, the free-end concrete is roughly divided into seven parts by splitting cracks and tensile cracks.

does not fully consider the yielding of the rockbolt [22, 23]. According to the load transfer process at the interface between the rockbolt and cement mortar in this study, the rockbolt yields but does not break in the pullout process. However, it is not difficult to find that the above model cannot fully describe the load transfer behaviour of rockbolts in the pullout process. The yielding of rockbolts will lead to the destruction of the grouted structure and endanger the safety of the roadway. Therefore, it is very important to study and consider the bond-slip model when the yielding of the rockbolt occurs.

When the value of L is 0 mm, according to the test results under the pullout load, the load at the interface between the rockbolt and the cement mortar undergoes four stages—elasticity, yielding, softening, and sliding, without
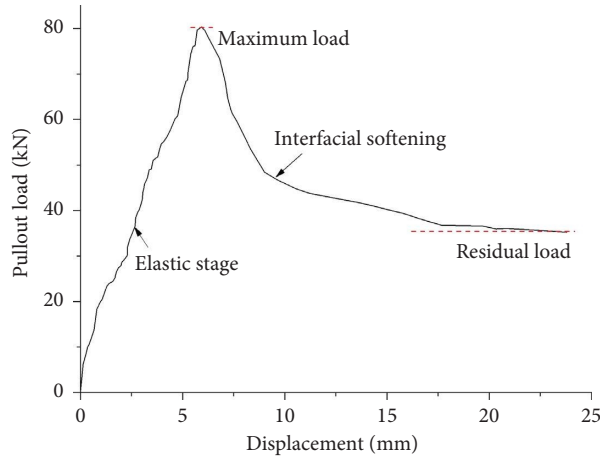
FIGURE 4: Axial load transfer behaviour on rockbolt when the value of L is 400 mm.
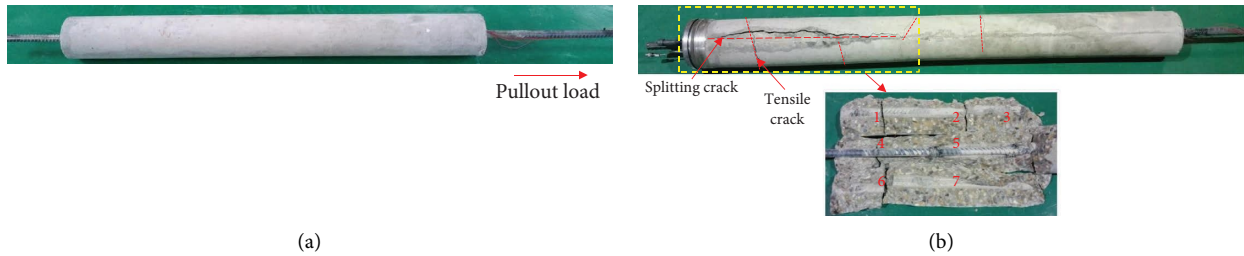

(a)

(b)

FIGURE 5: Failure modes of rockbolt grouted systems with different bond defect lengths. (a) The value of L is 400 mm. (b) The value of L is 0 mm.
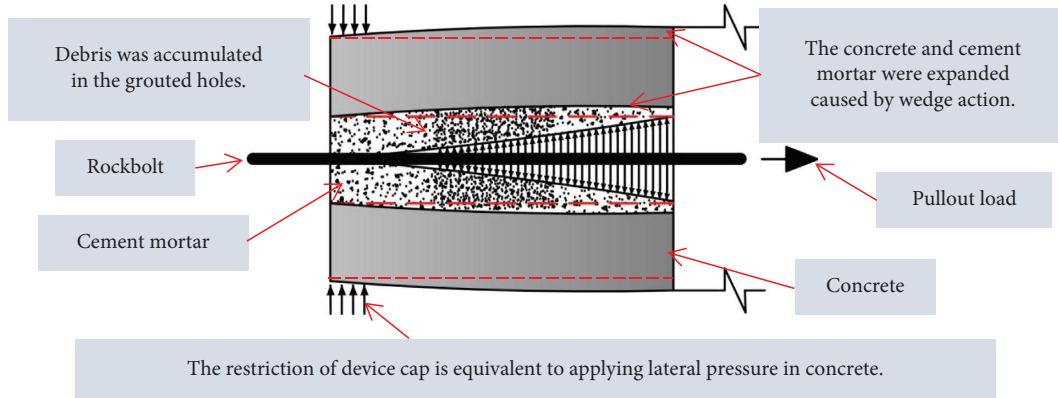

FIGURE 6: The state of cement mortar debris and typical stress distribution with lateral pressure [26].

fracture. The bond-slip relationship of a rockbolt can be simplified to a bond-slip model, o-a-b-c-d, as shown in Figure 7. Here, F_y, F_m, and F_r are the yield load, maximum load, and residual load of the rockbolt, respectively, and S_1, S_2, and S_3 are the corresponding displacements of F_y, F_m, and F_r.

In the o-a stage, the pullout load linearly increases with increasing displacement, and the bond-slip model can be described as follows:

$$F = F_y \frac{s}{s_1} \quad 0 \le s \le s_1. \tag{1}$$

In the a-b stage, the rockbolt begins to yield from point a. The simplified bond-slip relationship of the rockbolt at the yield stage is linear and can be described as follows:

$$F = F_y + \left(F_m - F_y\right) \frac{s - s_1}{s_2 - s_1} \quad s_1 \le s \le s_2. \tag{2}$$

FIGURE 7: The relationship of load-displacement of rockbolt when the value of L is 0 mm.
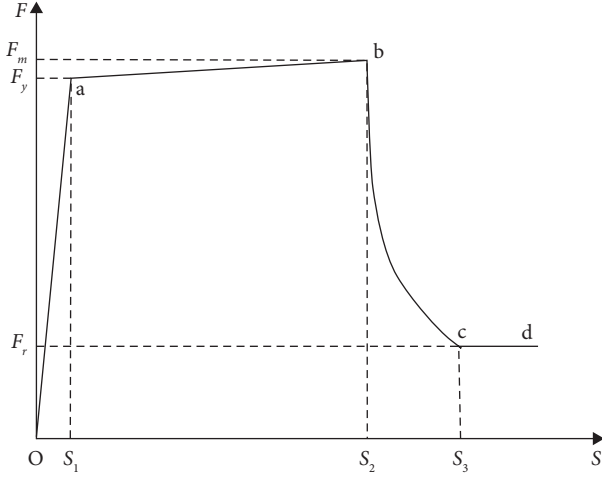

FIGURE 8: The relationship of load-displacement of rockbolt when the value of L is 400 mm.

In the b-c stage, the interface between the rockbolt and the cement mortar begins to soften, and in this stage, the load in the rockbolt decreases nonlinearly with increasing displacement. The bond-slip relationship can be described as follows:

$$F = F_m - (F_m - F_r)\left(\frac{s - s_2}{s_3 - s_2}\right)^\alpha \quad s_2 \leq s \leq s_3, \qquad (3)$$

where the value of α is a softening parameter, depending on the test results.

In stages c-d, the rockbolt has completely slipped at point c, and the load in the rockbolt does not change as the displacement increases. At this time, the load is the residual load, and the bond-slip relationship can be described as follows:

$$F = F_r \quad s_3 \leq s. \qquad (4)$$

Namely, the rockbolt undergoes four stages during the pullout process, and the bond-slip model expression can be summarized as follows:

$$\begin{cases} F = F_y\dfrac{s}{s_1} & 0 \leq s \leq s_1, \\[2mm] F = F_y + (F_m - F_y)\dfrac{s - s_1}{s_2 - s_1} & s_1 \leq s \leq s_2, \\[2mm] F = F_m - (F_m - F_r)\left(\dfrac{s - s_2}{s_3 - s_2}\right)^\alpha & s_2 \leq s \leq s_3, \\[2mm] F = F_r & s_3 \leq s. \end{cases} \qquad (5)$$

When the rockbolt does not yield in the pullout process, the load at the interface between the rockbolt and cement mortar undergoes three stages: elasticity, softening, and residual. The model in Figure 7 can be simplified to the bond-slip model o-a-b-c in Figure 8.
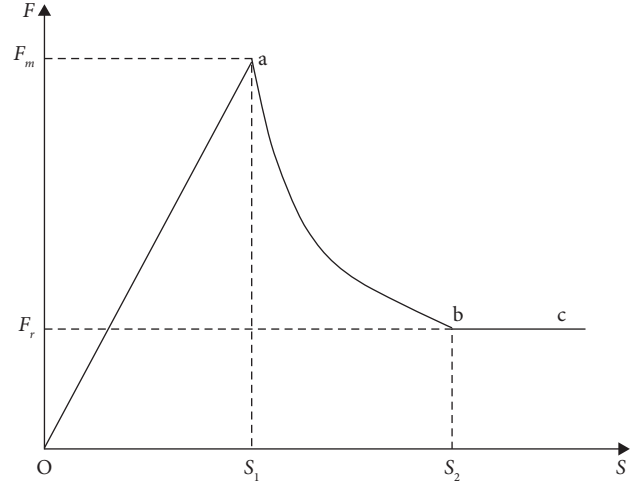
In the o-a stage, the expression of the bond-slip model is similar to equation (1), and the load increases linearly with increasing displacement.

In the a-b stage, the interface between the rockbolt and the cement mortar begins to soften, and the expression of the bond-slip model is the same as that in equation (3). The difference is that in the equation, F_y becomes F_r, S_3 becomes S_2, and S_2 becomes S_1. The expression of the bond-slip model is as follows:

$$F = F_m - (F_m - F_r)\left(\frac{s - s_1}{s_2 - s_1}\right)^\alpha \quad s_1 \leq s \leq s_2. \qquad (6)$$

In the b-c stage, the rockbolt has completely slipped, and the load in the rockbolt does not change with increasing displacement. The expression of the bond-slip model is the same as that in equation (4).

Because the rockbolt undergoes three stages in the pullout process, its bond-slip model expression can be summarized, and equation (5) can be simplified as follows:

$$\begin{cases} F = F_m\dfrac{s}{s_1} & 0 \leq s \leq s_1, \\[3mm] F = F_m - (F_m - F_r)\left(\dfrac{s - s_1}{s_2 - s_1}\right)^\alpha & s_1 \leq s \leq s_2, \\[3mm] F = F_r & s_2 \leq s. \end{cases} \qquad (7)$$

4.2. Test Verification. The bond-slip model proposed in this study is applied to compare and analyse the results of rockbolt pullout tests, and the results are shown in Figure 9. According to the test results, the value of α in equations (5) and (7) is 0.25. As shown in Figure 9(a), when the value of L is 0 mm, the rockbolt yields during the pullout process. The results calculated with the bond-slip model agree well with the experimental results, and they can accurately describe
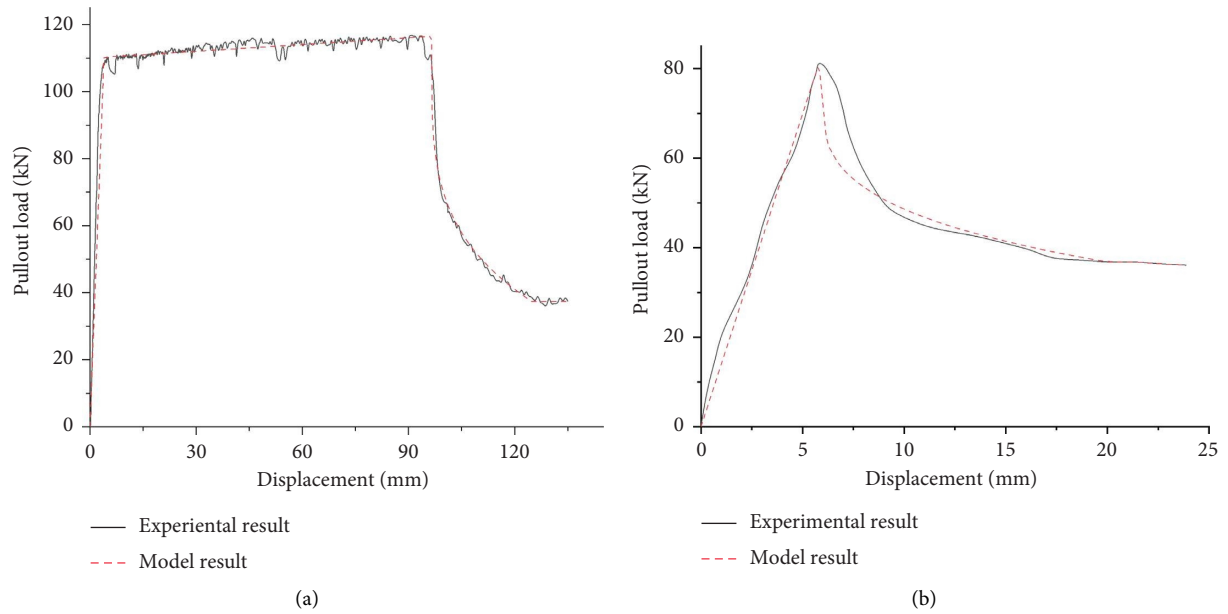
(a)

(b)

Figure 9: Comparison between model results and test results in this article. (a) The value of L is 0 mm. (b) The value of L is 400 mm.
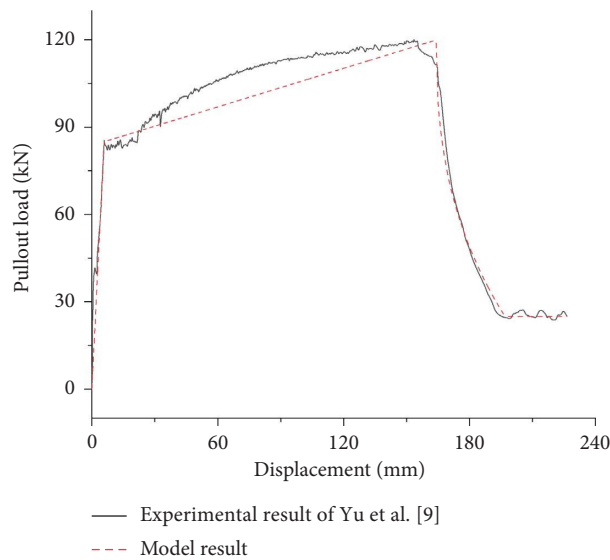

Figure 10: Comparison of model results with the experimental results of Yu et al. [9].

the elastic rise, yield, softening, and complete slip of the rockbolt during the pullout process. As shown in Figure 9(b), when the value of L is 400 mm, even if there is a bond defect, the calculated results of the bond-slip model and the test results are also relatively consistent. However, at the initial stage of interface softening, the model calculation results are relatively low compared to the test results, but the difference is not significant. The interface adhesion characteristics calculated based on the model can also accurately reflect the actual load transfer behaviour of the rockbolt in the test.

Figure 10 shows the load-displacement relationship of the grouted rockbolt systems with a rockbolt diameter of 18 mm and a bond length of 1500 mm under a pullout load

[9]. The figure shows that the rockbolt yielded but did not break. In the test results, $F_y = 84$ kN, $F_m = 120$ kN, $F_r = 25.1$ kN, $S_1 = 5.8$ mm, $S_2 = 153.5$ mm, and $S_3 = 192.1$ mm, and the value of α is 0.4. As shown in the figure, the model calculation results agree well with the test results, but in the yield stage, the model calculation value is lower than the test value. This is mainly due to the simplification of the bond-slip relationship of the rockbolt in the yield stage in the model to a linear relationship. This simplification underestimates the hardening phenomenon of the rockbolt in the yield stage, resulting in an increase in the rockbolt load. During the test, the influence of secondary factors was ignored, and the model was simplified. Therefore, there was a small error between the results calculated
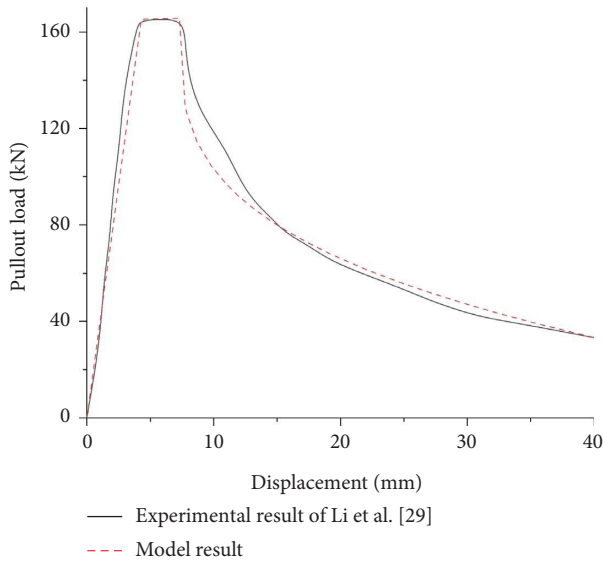
FIGURE 11: Comparison of model results with the experimental results of Li et al. [29].

using the model and the test results. The results of the calculation using the model were conservative, which was conducive to the safety of the structure.

Figure 11 shows the comparison between the model calculation results and the experimental results of Li et al. [29]. In the test, the bond length of the rockbolt was 200 mm, and the rockbolt also yielded. In the test results, $F_y = 162.9$ kN, $F_m = 165.9$ kN, $F_r = 33.3$ kN, $S_1 = 3.98$ mm, $S_2 = 7.29$ mm, and $S_3 = 40$ mm, and the value of α is 0.3 in equation (5). From the comparison results, it can be seen that the calculated results of the model agree well with the experimental results, which once again verifies that this model can accurately describe the load transfer behaviour of a rockbolt in the pullout process.

5. Conclusion

In this paper, the load transfer behaviour and failure mode of rockbolts were studied through experiments. Based on the load transfer process at the interface between the rockbolt and cement mortar, bond-slip models considering the nonyielding and yielding of rockbolts were proposed, and the following conclusions were obtained:

(1) When the value of L was 400 mm, the rockbolt was pulled out without yielding. When the value of L was 0 mm, with an increase in the pulling load, chemical adhesion and mechanical interlocking were fully mobilized and acted on the grouted rockbolt systems. The rockbolt yielded but did not break.

(2) When the value of L was 0 mm, the rockbolt was pulled out, accompanied by partial splitting failure of the concrete parallel to the rockbolt direction and tensile failure of the concrete perpendicular to the rockbolt direction. Due to the effect of the wedge action, cement mortar debris were collected in the interior of the grouted rockbolt systems. As a result,

radial pressure exceeded the tensile strength of the concrete, and internal cracks rapidly initiated and expanded to the concrete surface. The free end of the grouted rockbolt system was limited by the equipment end cap, which hindered the radial expansion of the concrete and led to the formation of splitting cracks and tensile cracks in the middle of the concrete.

(3) Based on the established bond-slip model that considers the yielding of the rockbolt, the calculated characteristics of interfacial adhesion could accurately reflect the actual load transfer behaviour of the rockbolt in the test. For the test results of Yu et al. [9], during the yield stage, the value calculated using the model was less than the experimental value. This was mainly due to the simplified linear relationship in the model, which underestimated the hardening behaviour of the rockbolt, resulting in an increase in the load.

Data Availability

The data used to support the findings of this study are included within the article.

Conflicts of Interest

The authors declare that there are no conflicts of interest.

References

[1] A. Bobet and H. H. Einstein, "Tunnel reinforcement with rockbolts," *Tunnelling and Underground Space Technology*, vol. 26, no. 1, pp. 100–123, 2011.

[2] Z. Y. Sun, D. L. Zhang, Q. Fang, D. P. Liu, and G. S. Dui, "Displacement process analysis of deep tunnels with grouted rockbolts considering bolt installation time and bolt length," *Computers and Geotechnics*, vol. 140, Article ID 104437, 2021.

[3] A. J. S. Spearing, A. J. Hyett, T. Kostecki, and M. Gadde, "New technology for measuring the in situ performance of rock bolts," *International Journal of Rock Mechanics and Mining Sciences*, vol. 57, pp. 153–166, 2013.

[4] B. I. Bae, H. K. Choi, and C. S. Choi, "Bond stress between conventional reinforcement and steel fibre reinforced reactive powder concrete," *Construction and Building Materials*, vol. 112, pp. 825–835, 2016.

[5] E. Luga and E. Periku, "A pioneer in-situ investigation on the bearing capacity and failure causes of real scale fully grouted rockbolts," *Construction and Building Materials*, vol. 310, Article ID 124826, 2021.

[6] I. Thenevin, L. Blanco-Martín, F. Hadj-Hassen, J. Schleifer, Z. Lubosik, and A. Wrana, "Laboratory pull-out tests on fully grouted rock bolts and cable bolts: results and lessons learned," *Journal of Rock Mechanics and Geotechnical Engineering*, vol. 9, no. 5, pp. 843–855, 2017.

[7] A. Teymen and A. Kilic, "Effect of grout strength on the stress distribution (tensile) of fully-grouted rockbolts," *Tunnelling and Underground Space Technology*, vol. 77, pp. 280–287, 2018.

[8] S. Khaleghparast, N. Aziz, A. Remennikov, and S. Anzanpour, "An experimental study on shear behaviour of fully grouted rock bolt under static and dynamic loading conditions," *Tunnelling and Underground Space Technology*, vol. 132, Article ID 104915, 2023.

[9] S. S. Yu, W. C. Zhu, L. L. Niu, S. C. Zhou, and P. H. Kang, "Experimental and numerical analysis of fully grouted long rockbolt load-transfer behavior," *Tunnelling and Underground Space Technology*, vol. 85, pp. 56–66, 2019.

[10] D. P. Xu, Q. Jiang, S. J. Li, S. L. Qiu, S. Q. Duan, and S. L. Huang, "Safety assessment of cable bolts subjected to tensile loads," *Computers and Geotechnics*, vol. 128, Article ID 103832, 2020.

[11] J. M. Hawkes and R. H. Evans, "Bond stresses in reinforced concrete columns and beams," *Journal of the Institute of Structural Engineers*, vol. 10, no. 24, pp. 323–327, 1951.

[12] B. Benmokrane, A. Chennouf, and H. S. Mitri, "Laboratory evaluation of cement-based grouts and grouted rock anchors," *International Journal of Rock Mechanics and Mining Sciences & Geomechanics Abstracts*, vol. 32, no. 7, pp. 633–642, 1995.

[13] M. Monti, M. Renzelli, and P. Luciani, "FRP adhesion in uncracked and cracked concrete zones," in *Proceedings of 6th International Symposium on FRP Reinforcement for Concrete Structures*, pp. 183–192, World Scientific Publications, Singapore, 2003.

[14] G. Trabacchin, W. Sebastian, and M. Z. Zhang, "Experimental and analytical study of bond between basalt FRP bars and geopolymer concrete," *Construction and Building Materials*, vol. 315, Article ID 125461, 2022.

[15] F. F. Ren, Z. J. Yang, J. F. Chen, and W. W. Chen, "An analytical analysis of the full-range behaviour of grouted rockbolts based on a tri-linear bond-slip model," *Construction and Building Materials*, vol. 24, no. 3, pp. 361–370, 2010.

[16] D. J. Shen, X. Shi, H. Zhang, X. F. Duan, and G. Q. Jiang, "Experimental study of early-age bond behavior between high strength concrete and steel bars using a pull-out test," *Construction and Building Materials*, vol. 113, pp. 653–663, 2016.

[17] J. Zhou, J. J. Xu, J. M. Cong et al., "Optimization for quick, easy, cheap, effective, rugged and safe extraction of mycotoxins and veterinary drugs by response surface methodology for application to egg and milk," *Journal of Chromatography A*, vol. 1532, pp. 20–29, 2018.

[18] W. L. Zhang, L. Huang, and C. H. Juang, "An analytical model for estimating the force and displacement of fully grouted rock bolts," *Computers and Geotechnics*, vol. 117, Article ID 103222, 2020.

[19] J. Y. Han, D. Liu, Y. P. Guan et al., "Study on shear behavior and damage constitutive model of tendon-grout interface," *Construction and Building Materials*, vol. 320, no. 3, Article ID 126223, 2022.

[20] X. Y. Xiong, L. Y. He, Z. W. Zhou, and Q. S. Xiao, "The bond-slip constitutive model of retard-bonded prestressing steel strand," *Construction and Building Materials*, vol. 365, Article ID 129995, 2023.

[21] C. Kong, T. Yang, M. Xiao, and Q. T. Yuan, "Numerical simulation of fully grouted rock bolts with or without faceplates based on the tri-linear bond-slip model," *Construction and Building Materials*, vol. 367, Article ID 130288, 2023.

[22] Z. W. Yue, A. Li, P. Wang, and P. Wang, "An analytical analysis for the mechanical performance of fully-grouted rockbolts based on the exponential softening model," *International Journal of Mining Science and Technology*, vol. 32, no. 5, pp. 981–995, 2022.

[23] Y. X. Chen, Y. F. Zhao, L. Zeng, W. X. Zhang, and T. Yang, "Bond performance and bond-slip constitutive model for rebar embedded in rubber powder-modified polypropylene fiber reinforced concrete," *Construction and Building Materials*, vol. 375, Article ID 130934, 2023.

[24] S. S. Yu, L. L. Niu, J. Chen, Y. W. Wang, and H. H. Yang, "Study on bond defect detection in grouted rock bolt systems under pullout loads," *Advances in Materials Science and Engineering*, vol. 2022, Article ID 3282211, 9 pages, 2022.

[25] S. S. Yu, W. C. Zhu, and L. L. Niu, "Experimental and numerical evaluation on debonding of fully grouted rockbolt under pull-out loading," *International Journal of Coal Science & Technology*, vol. 9, no. 1, p. 8, 2022.

[26] H. M. Afefy and E. T. M Ei-Tony, "Bond behaviour of embedded reinforcing steel bars for varying levels of transversal pressure," *Journal of Performance of Constructed Facilities*, vol. 30, no. 2, 2015.

[27] P. K. Kaiser, S. Yazici, and J. Nose, "Effect of stress change on the bond strength of fully grouted cables," *International Journal of Rock Mechanics and Mining Sciences & Geomechanics Abstracts*, vol. 29, no. 3, pp. 293–306, 1992.

[28] A. Kilic, E. Yasar, and C. D. Atis, "Effect of bar shape on the pull-out capacity of fully-grouted rockbolts," *Tunnelling and Underground Space Technology*, vol. 18, pp. 1–6, 2003.

[29] C. C. Li, G. Kristjansson, and A. H. Hoien, "Critical embedment length and bond strength of fully encapsulated rebar rockbolts," *Tunnelling and Underground Space Technology*, vol. 59, pp. 16–23, 2016.